# A Limited Effect of Sub-Tropical Typhoons on Phytoplankton Dynamics

Fei Chai[1,2*], Yuntao Wang[1], Xiaogang Xing[1], Yunwei Yan[1], Huijie Xue[2,3], Mark Wells[2], Emmanuel Boss[2]

[1] State Key Laboratory of Satellite Ocean Environment Dynamics, Second Institute of Oceanography, Ministry of Natural Resources, Hangzhou, 310012, China

[2] School of Marine Sciences, University of Maine, Orono, ME, 04469, USA

[3] State Key Laboratory of Tropical Oceanography, South China Sea Institute of Oceanology, Chinese Academy of Sciences, Guangzhou, 510301, China

*Correspondence to* Fei Chai (fchai@sio.org.cn)

**Abstract.** Typhoons are assumed to stimulate ocean primary production through the upward mixing of nutrients into the surface ocean, based largely on observations of increased surface chlorophyll concentrations following the passage of typhoons. This surface chlorophyll enhancement, seen on occasion by satellites, more often is undetected due to intense cloud coverage. Daily data from a BGC-Argo profiling float revealed the upper-ocean response to Typhoon Trami in the Northwest Pacific Ocean. Temperature and chlorophyll changed rapidly, with a significant drop in sea surface temperature and surge in surface chlorophyll associated with strong vertical mixing, which was only partially captured by satellite observations. However, no net increase in vertically integrated chlorophyll was observed during Typhoon Trami or in its wake. Contrary to the prevailing dogma, the results show that typhoons likely have limited effect on net ocean primary production. Observed surface chlorophyll enhancements during and immediately following typhoons in tropical and subtropical waters are more likely associated with surface entrainment of deep chlorophyll maxima. Moreover, the findings demonstrate that remote sensing data alone can overestimate the impact of storms on primary production in all oceans. Full understanding of the impact of storms on upper ocean productivity can only be achieved with ocean observing robots dedicated to high-resolution temporal sampling in the path of storms.

## 1 Introduction

The western North Pacific Ocean is a highly energetic region on the globe (Gray, 1968), where nearly one third of the tropical cyclones originate (Needham et al., 2015). The strong tropical cyclones in this region, referred to as typhoons, are highly dangerous and have caused great losses of lives and property throughout history (Frank and Husain, 1971; Dunnavan and Diercks, 1980; Kang et al., 2009; Needham et al., 2015). Typhoons extract their energy from warm surface ocean waters, thus the heat content in the upper ocean (with the sea surface temperature (SST) as the indicator) has a key role in development of typhoons (Emanuel, 1999). Increasing SST in the North Pacific over the past few decades (He and Soden, 2015) coincided with an increase in the number of intense typhoons in the region (Emanuel, 2005; Webster et al., 2005; Vecchi et al., 2007;

Kossin, 2018), which has been found to relate with climate change (Mei et al., 2015). The trend draws public attention for its potential influence on increasing climate extremes in this region.

35   Numerous studies have analysed the impact of typhoons on upper-ocean conditions (e.g., Sun et al., 2010; Zhang et al., 2018). Higher surface ocean temperatures enhance stratification and thus decrease the nutrient flux, which reduces the ability of typhoon to cool the upper ocean and limits the growth of phytoplankton (Zhao et al., 2017). The ocean productivity and carbon sequestration are subsequently reduced, resulting in a negative response proposed to facilitate continued global temperature increase (Balaguru et al., 2016). The high winds and strong energy exchange associated with typhoons (Price, 1981), on the other hand, are suggested to partially reverse this trend by mixing subsurface cold and nutrient-rich water into the sunlit surface

40   layer (Babin et al., 2004), which results in decreasing SST and enhanced phytoplankton growth at the ocean surface (Platt, 1986, Ye et al., 2013).

The feedback from ocean to typhoon is important for the development and maintenance of typhoons, as the requires extracting energy from ocean surface (Zheng et al., 2008). The translation speed, e.g., moving speed of typhoon, plays an important role

45   in determining the interaction between ocean surface and typhoon (Pothapakula et al., 2017). The typhoon can lose energy and get weak when passing over cold surface, e.g., in regions with cooling induced by a typhoon itself; thus, slow moving typhoons can hardly develop into a stronger one (Lin et al., 2009). On the other hand, the longer enforcing time when typhoon lingers around certain location allows the typhoon to exert stronger impact (Zhao et al., 2013); the resulted cooling further damps the intensity of typhoon. Thus, strong typhoons, e.g., category 4 or 5, in mid-latitude regions are generally characterized as fast

50   moving and strong typhoons (Lin, 2012).

As typhoons propagate, they can drive substantial mixing and upwelling to influence the upper ocean (Han et al., 2012). Typhoon induced mixing lasted for a week or so with an impact from the surface up to 100 m (Price, 1994), while the upwelling took place for only half day but over a great depth, e.g., 200 m or more (Zhang et al., 2018). Thus, the mixing is much more

55   effective for inducing ocean surface changes comparing with upwelling (Jacob, 2000). Mixing acts to deepen the mixed layer depth, resulting in a redistribution of ocean surface variables (Lin et al., 2017). For typhoons passing over via regions with shallow water-depth and strong stratification, large ocean surface responses are generally observed (Zhao et al., 2017).

There is a strong linkage among the stratification in the upper ocean, chlorophyll distribution, and nutricline in mid latitude

60   regions, where any intensification of vertical mixing often leads to a surge in nutrient flux to surface waters. But the same linkage is not necessarily true in tropical and subtropical regions, where a two-stratum sunlit "surface" layer forms. Here the wind-mixed layer comprises only the upper (shallow) portion of the sunlit, and nutrient-depleted surface layer, with the former being much shallower than the latter (Du et al., 2017). Whereby the photic zone extends far below the typical wind-mixed layer, a deep chlorophyll maximum (DCM) forms at the top of nutricline that may exist at twice or more the depth of the wind-

65   mixed layer (Letelier et al., 2004; Cullen 2015; Gong et al., 2017; Pan et al., 2017). The question then is whether the energy transfer from typhoons generates sufficient mixing to "break" through both the base of the wind-mixed layer as well as the deeper nutricline, thereby transfer new nutrients into the photic zone. Typhoon induced upwelling can inject nutrient into mixed layer, which can introduce a subsurface chlorophyll enhancement where the upwelling prevails (Ye et al., 2013).

70   Besides the intensive wind field, typhoons are also associating with intensified rainfall and cloud (Liu et al., 2013), which can substantially contaminate satellite observations. Satellite-based studies occasionally capture the ocean surface feature during the passage of typhoon and offer more dataset at the wake following typhoons (Chang et al., 2008). Remote sensing data revealed that the SST rapidly decreases during typhoon passage, whereas chlorophyll can increase afterwards (Chen and Tang, 2012; Zhao et al., 2017). It was suggested that the delayed response of surface chlorophyll is related to the growth time needed

75   for phytoplankton to exploit the increased nutrient concentrations (Chen et al., 2014).

Typhoon induced ocean responses are largely varying in intensity and even magnitude of changes depending on the typhoon's feature and ocean state. Slow and strong typhoons are favourable for inducing the oceanic responses (Lin et al., 2017), which can be amplified by pre-existing cyclonic eddies (Sun et al., 2010). Bauer and Waniek (2013) showed that individual typhoons

80   may more than double the surface primary production. On the other hand, Zhao et al. (2008; 2017) found that only strong and slow-moving typhoons impart sufficient energy to increase surface chlorophyll concentrations. The diverse outcomes observed among typhoons and upper ocean interactions (Chang et al., 2008; Chen and Tang, 2012; Balaguru et al., 2016) illustrate the incomplete understanding of how typhoons may affect the primary productivity in the present and future ocean.

## 2 Methods

85   ### 2.1 Data used in this study

The BGC-Argo profiling float (ID: 2902750) was deployed by the State Key Laboratory of Satellite Ocean Environment Dynamics (SOED) of China, in early September of 2018 in the Northwest Pacific (South of Japan). It was equipped with a CTD ("SBE41CP" manufactured by Seabird) measuring temperature and salinity, and an optical sensor package ("ECO Triplet" manufactured by WET Labs) measuring chlorophyll-a concentration (Chla; mg/m$^{-3}$), fluorescent dissolved organic

90   matter (FDOM; ppb) and particulate backscattering coefficient at 700 nm (bbp-700; m$^{-1}$). Measurements were made every night (around 22:00 local time) to avoid in-vivo fluorescence non-photochemical quenching, with ~ 1 m vertical resolution in the upper 1000 m.

Float data passed through a computer-based real-time quality control (RTQC) and were subsequently uploaded to the Argo

95   global data assembly center (GDAC). Data used in this study are available at from the Coriolis GDAC FTP server (Argo, 2020). Chla and bbp (700) profiles were smoothed with 5-point median filter, and their factory-calibrated dark counts (48 and

48) were replaced by the on-float-measured counts (50 and 53), which were measured by the sensors on the float before deployment.

100   The remote sensing observations of SST and sea surface chlorophyll are obtained as the MODIS L3 daily data. The spatial resolution is 1/24° and there is no data presenting over land or cloud. Satellite observed information near BGC-Argo was calculated by spatially averaging over the region less than 300km around, excluding those within 10km from the land.

## 2.2 MLD and mixing-induced changes in MLT and MLC

105   Following Kara et al. (2000), the estimate of MLD was obtained using a density-based criterion with the increment in density equivalent to the decrease in temperature by 0.8°C from the ocean surface. On September 30, a sublayer formed above the mixed layer. To correctly reflect ocean turbulence mixing on that day, the sublayer was ignored when calculating the MLD. MLT and MLC were simply the vertically averaged temperature and chlorophyll concentration from the surface to the MLD. We further defined and calculated the mixing-induced change in MLT in a daily interval using the following Eq. (1):

110   $$\Delta\text{MLT}_{\text{m}} = \left.\int_0^h \rho_r C_p T_0 dz \middle/ \rho_r C_p h\right. - \left.\int_0^{h_0} \rho_r C_p T_0 dz \middle/ \rho_r C_p h_0\right. = \left.\int_0^h T_0 dz \middle/ h\right. - \left.\int_0^{h_0} T_0 dz \middle/ h_0\right. \tag{1}$$

where $\Delta\text{MLT}_{\text{m}}$ is mixing-induced change in MLT, $\rho_r$ is the relative water density, $C_p$ is the specific heat capacity at constant pressure, $h$ is the MLD, $h_0$ and $T_0$ is, respectively, the MLD and temperature in the previous day. Mixing-induced change in MLC was calculated similarly.

## 3 Results

115   We recently obtained unique observations of the effect of a strong typhoon on the upper ocean using data collected from a biogeochemical-Argo (BGC-Argo) float, an unmanned observational platform (Bishop et al., 2002; Boss et al., 2008; Claustre et al., 2010; Mignot et al., 2014; Chacko, 2017). Besides measuring temperature and salinity, the float was also equipped with an optical sensor package measuring chlorophyll-a concentration, fluorescent dissolved organic matter and particulate backscattering coefficient. The category 5 typhoon Trami was spawned in the tropical western Pacific in late September 2018

120   and moved from the tropics to the mid-latitudes around Japan with overall translation speed equalled to 6.1 ± 6.5 m/s (Figure 1). Typhoon Trami passed over the BGC-Argo float (2902750) on September 30 while it was sampling daily from 1000 m depth to the surface at 10m intervals. Corresponding daily-averaged translation speed was 19.3 ± 6.1 m/s indicating the typhoon was moving faster on September 30 comparing with other time during its lifespan.

125   The BGC-Argo float profiles, along with remote sensing data, show a rapid drop in surface water temperatures above the base of the mixed-layer depth (MLD) and warming below it, associated with a swift deepening of the mixed layer upon passage of

the typhoon (Figure 2a, b). The largest reduction of SST (> 1°C) happened simultaneously with arrival of the typhoon, consistent with the local shear-driven vertical mixing mechanism (Sriver and Huber, 2007; Chang et al., 2008; Zhao et al., 2008; Sanford et al., 2011).

130

The changes in vertical distribution of chlorophyll were equally striking, with the DCM decreasing from 0.8 to 0.4 mg chl a/m$^3$ while near-surface values more than doubled (Figure 2b, c). We observed two surface chlorophyll peak values on September 30 and October 3, at 0.18 and 0.15 mg chl a/m$^3$, respectively. These increases represent changes of 0.13 and 0.08 mg chl a/m$^3$, respectively, above the concentration measured on September 29 before the typhoon approached to the area. The highest value occurred on September 30 when the surface wind peaked around the BGC-Argo float, which supports the vertical mixing mechanism. This enhancement was, however, not captured by satellite remote sensing due to intense cloud coverage from the typhoon.

Our results suggest the mixing to be the most dominant process during the typhoon passage. The MLD deepened dramatically from 40 m to 94 m (Figure 3a) as the wind speed peaked on September 30. While the mixed-layer temperature (MLT) decreased quickly, the integrated ocean heat content (OHC) of the top 150 m remained relatively constant around 1.47 J/m$^2$ (Figure 3b). The elevated the mixed-layer chlorophyll concentration (MLC) coincided with decreasing concentrations at DCM (Figure 3c). As a consequence, the strong vertical mixing generated no increase in the depth-integrated chlorophyll within the upper 150-m either during or after the passage of Typhoon Trami (Figure 3d). There was no increase measured in particle backscatter coefficient (bbp) that correlates well with phytoplankton carbon (Graff et al., 2015), suggesting there was no significant change in phytoplankton abundance or any shift towards larger phytoplankton that might enhance carbon export.

The calculated profiles of temperature and chlorophyll change are shown in Figure 4a and 4b. The temperature above 50 m decreased with the largest reduction near the surface, while the temperature beneath increased simultaneously. This process was fully captured as Trami approached till six days later. The largest temperature increase happened between 75 and 100 m from September 30 to October 3 when the surface temperature dropped prominently, which indicated the heat exchange between the surface and subsurface layers. Consistently, the time series of chlorophyll profiles depicted the typhoon-induced chlorophyll enhancement near the surface and decrease below. Because the initial vertical gradient of chlorophyll was very low in the upper 50 m, the increase was mainly uniform throughout the upper 50 m. The largest decrease of chlorophyll was observed around 110-m depth where the initial DCM was located. This pattern is consistent with that from shipboard observations, which found a strong vertical movement of particles in the subsurface layer rather than at the surface (Ye et al., 2013).

We calculated the mixing-induced daily change in mixed-layer temperature and chlorophyll ($\Delta MLT_m$ and $\Delta MLC_m$, see the definition in Methods section) and compared them with the daily change in sea surface temperature (SST) and sea surface

chlorophyll (SSC) from the BGC-Argo float data ($\Delta$SST and $\Delta$SSC) (Figure 4c). The observed surface change in temperature was predominantly attributable to strong wind mixing during the typhoon passage. The calculated $\Delta$MLT$_m$ of 1.8°C on September 30 was in close agreement with $\Delta$SST, consistent with the strong mixing scenario. Similarly, there was a close agreement between the observed SSC and calculated $\Delta$MLC$_m$ that matched the peak on September 30, which indicates the strong vertical mixing contributes surface chlorophyll increase.

## 4 Discussion

The passage of typhoon over BGC-Argo offers a unique opportunity to fully resolve the typhoon induced ocean surface responses. In contrary to interpretation of remote sensing data, the super Typhoon Trami did not significantly boost phytoplankton biomass or production in the upper ocean, and that the measured increases in near-surface chlorophyll concentrations resulted simply from the redistribution of phytoplankton, originally residing in the deep chlorophyll maximum, across the mixed layer now reaching throughout the photic zone, as summarized in Figure 5. Moreover, the implication is that we often overestimate typhoon-induced change of primary production based on satellite observations alone, unless consideration is given to chlorophyll redistribution in the water column.

Typhoon-induced mixing predominated the variability of surface chlorophyll during the passage of Trami, which leads to the redistribution of chlorophyll within the upper ocean (Figure 3c). In many of the former remote sensing studies, typhoons are thought to boost primary production via introducing nutrients from deep ocean via upwelling (e.g., Chen and Tang, 2012). And the peak of chlorophyll is usually reached few days after the minimum SST because the time required for the growth of phytoplankton (Shang et al., 2008). However, with the in-situ BGC-Argo profiling at high-frequency, the results show almost no changes of temperature and chlorophyll in upper ocean that the integrated values within top 150 meter are mostly constant (Figure 3d). Also, the upward displacement of isotherm is only observed for the upper ocean less than 100 meter (Figure 2a) where upwelling is usually found throughout water column extending more than 200m (Ye et al., 2013). The results indicate mixing is much stronger than upwelling and suggest the importance of comparing typhoon-induced mixing depth, thermocline and nutricline when discussing the upper ocean's responses to typhoons. A net decreasing in heat content and increasing in primary production can only be achieved if typhoon penetrate through the thermocline and nutricline, respectively (Zhang et al., 2018). Consistently, stronger typhoon induced responses are found in pre-existing cyclonic eddies where stratification is elevated by upwelling (Zheng et al., 2008; Wu and Li, 2018).

As the mixing process dominated the dynamics in ocean surface, the impact of typhoon happened and faded quickly during and after typhoon, respectively (Figure 2d). The chlorophyll rapidly relaxed to initial value within five days after typhoon attributing to consumption of nutrient (Shibano et al., 2011) and intensive grazing (Zhou et al., 2011; Chung et al., 2012). In comparison, the temperature raises up slowly associating with the gradual deepening of MLD and increasing in stratification

(Figure 2a). This is at least attribute to the solar radiation is much weaker comparing with tropics where the SST and stratification rebound quickly after passage of a typhoon (Gierach and Subrahmanyam, 2008).

195

The position of BGC-Argo is locating roughly 200km away from the land; thus, typhoon induced rainfall may increase nutrient loading from land and influence the growth of phytoplankton (Zheng and Tang, 2007). Typhoon induced surface advection can extend southward from the coast of Japan for more than 100km (Yang et al., 2010); thus, it is important to consider whether the coastal process can influence the location of BGC-Argo. In current study, only satellite observations more than 10km from

200 the land and less than 300km within BGC-Argo are included, and the daily-averaged satellite data is not largely varying with the spatial range (Figure 1). The terrestrial impact induced by intensive rainfall is not prominent for the region around BGC-Argo, which is different comparing with many estuaries, e.g. Pearl River Estuary, where the rainfall associated with typhoon can substantially introduce nutrients and river discharge in the coastal region (Zheng and Tang, 2007).

205 Typhoon Trami is characterized as a strong and fast-moving typhoon with large wind intensity and translation speed (Wu and Li, 2018), which are favorable for inducing prominent changes in ocean surface (Pothapakula et al., 2017). There is almost no lingering during its propagation and the ahead cooling induced by itself is not largely impacting the intensity (Glenn et al., 2016). Indeed, the ocean surface cooling and bloom are indeed identified along the track of typhoon (Figure 1a), in particular, to the right-side. The BGC-Argo float was located on the right-hand side of Typhoon Trami's passage, often believed to be

210 subject to more energetic mixing (e.g., Babin et al., 2004; Glenn et al., 2016), although Huang and Oey (2015) showed only weak asymmetry in mixing across storms.

The decreasing in SST is a general pattern; in comparison, the typhoon induced variation in chlorophyll is much more complex and varying in each case. Increasing in chlorophyll are found respective only around 50% and 18% of typhoons in the South

215 China Sea (Pan et al., 2017) and northwest Pacific Ocean (Lin, 2012). This is at least due to the surface observations can only observe an elevation in chlorophyll if vertical mixing reaches DCM (Figure 2) or upwelling reaches the surface (Zhang et al., 2018). In terms of satellite, a measurement with less cloud coverage is required; however, it is usually not the case during the passage of typhoons (Chen and Tang, 2012). The BGC-Argo measures vertical profiles that can be helpful to determine whether a net increasing in primary production, e.g., nutrient injection to upper ocean or subsurface bloom (Ye et al., 2013),

220 taking place.

The findings here have a broad application for assessing the impact of typhoons on global primary production and carbon cycling. An increasing trend of super typhoons (Elsner et al., 2008; Sobel et al., 2016) may subject the coastal and shelf regions to a larger biogeochemical alteration, but they are much less effective in boosting oceanic productivity where the nutricline is

225 deeper and thus more sheltered from enhanced vertical transport. Re-examination of past storm events in this context is necessary to better quantify changes in primary production, but our findings imply that future increases in storm frequency

alone are unlikely to mitigate the declining trend in global phytoplankton biomass resulted from the enhanced stratification due to warming (Boyce et al., 2010; Lin and Chan, 2015).

230    The BGC-Argo floats typically provide three-dimensional observations at a 10-day profiling cycle to extend their operational lifetimes (Johnson and Claustre, 2016), a sampling frequency too low to capture synoptic weather and other short-term events. Near-daily sampling frequencies, on the other hand, are better to inform on rapid processes in response to short-term atmospheric perturbations. Combined with high-frequency remote sensing data, these observations would enable the development of new and more comprehensive conceptual and quantitative models to improve our understanding of how 235    climate drivers will influence ocean primary production and the associated carbon export in future oceans.

## 5 Conclusions

Unique observational dataset from daily BGC-Argo profiles offers a great opportunity to examine the impact of typhoon on the upper ocean. The daily profiling frequency allows to capture the rapid responses of ocean surface to typhoon Trami. The results clearly show mixing is overwhelming the dynamics comparing with the upwelling, which was formerly identified to 240    be important for many typhoons. The observed surface phytoplankton increase is actually attributed to mixing in upper ocean, e.g., redistribution of DCM over the mixed layer; however, there is no net increasing in primary production. In many studies conducted via satellite observations, the delayed bloom that induced by typhoons may be due to the cloud coverage during the passage of typhoon. Thus, it implies an underestimation for the typhoon induced mixing and its associated vertical redistribution of water masses, while the impact of nutrients that being injected into euphotic zone can be overestimated.

245

The cutting-edge observational platforms, e.g., BGC-Argo and other mobile unmanned surface vehicles, are prominently important for resolving episodic climatic events and deliver new information that haven't been fully resolved by traditional observations. The Argo profiling at each 10 days can easily miss the daily or weekly variability induced by typhoons, and an automatically adjusting system, which can change the sampling frequency based on the duration of targeted events (Chai et 250    al., 2020), can be important to improve the impact of typhoons on marine system.

*Acknowledgements*. The BGC-Argo float data used for this study can be downloaded from ftp://ftp.ifremer.fr/ifremer/argo. Satellite observation files are available from the NASA database (podaac-tools.jpl.nasa.gov/drive/files/allData/modis). The authors appreciate the Argo and Biogeochemical Argo program, and NASA for sharing the data

255

*Author contributions*. F. C. designed the observational plan, interpreted the data, and wrote the manuscript; Y. W. organized the figures and results, and worked on the draft; X. X. and Y. Y. conducted the data analysis; H. X., M. W., and E. B. provided insightful comments and improve the manuscript.

260    *Financial support.* This research was supported by the National Key Research and Development Program of China under
contract 2016YFC1401600, the National Natural Science Foundation of China under contracts 41730536 and 41890805.

## References

Argo (2020). Argo float data and metadata from Global Data Assembly Centre (Argo GDAC). *SEANOE*.
https://doi.org/10.17882/42182

265    Babin, S. M., Carton, J. A., Dickey. T. D. and Wiggert, J. D.: Satellite evidence of hurricane induced phytoplankton blooms
in an oceanic desert. J. Geophys. Res., 109, C03043, 2004.

Balaguru, K., Foltz, G. R., Leung, L. R. and Emanuel, K. A.: Global warming-induced upper-ocean freshening and the
intensification of super typhoons. Nature Communications, 7, 13670, 2016.

Bauer, A. and Waniek, J. J.: Factors affecting chlorophyll a concentration in the central Beibu Gulf, South China Sea. Mar.
270        Ecol. Prog. Ser., 474, 67–88, 2013.

Bishop, J. K. B., Davis, R. E. and Sherman, J. T.: Robotic observations of dust storm enhancement of carbon biomass in the
North Pacific. Science, 298, 817–821, 2002.

Boss, E., Swift, D., Taylor, L., Brickley, P., Zaneveld, R., Riser, S., Perry, M. J. and Strutton, P. G.: Observations of pigment
and particle distributions in the western North Atlantic from an autonomous float and ocean color satellite. Limnol.
275        Oceanogr., 53, 2112–2122, 2008.

Boyce, D. G., Lewis, M. R. and Worm, B.: Global phytoplankton decline over the past century. Nature, 466, 591–96, 2010.

Chacko, N.: Chlorophyll bloom in response to tropical cyclone Hudhud in the Bay of Bengal: Bio-Argo subsurface
observations. Deep-Sea Res. I, 124, 66–72, 2017.

Chai, F., Johnson, K. S., Claustre, H., Xing, X., Wang, Y., Boss, E., Riser, S., Fennel, K., Oscar Schofield, O., Sutton, A.:
280        Monitoring ocean biogeochemistry with autonomous platforms, Nature Reviews Earth & Environment, 1, 315–326,
2020.

Chang, Y., Liao, H. T., Lee, M. A., Chan, J. W., Shieh, W. J., Lee, K. T., Wang, G. H. and Lan, Y. C.: Multisatellite observation
on upwelling after the passage of Typhoon Hai-Tang in the southern East China Sea. Geophys. Res. Lett., 35, L03612,
2008.

285    Chen, C. and Tang, D.: Eddy-feature phytoplankton bloom induced by a tropical cyclone in the South China Sea. Int. J. Remote
Sens., 33, 7444–7457, 2012.

Chen, G, Xiu, P. and Chai, F.: Physical and biological controls on the summer chlorophyll bloom to the east of Vietnam. J.
Oceanogr., 70, 323–328, 2014.

Chung, C., Gong, G., and Hung, C.: Effect of Typhoon Morakot on microphytoplankton population dynamics in the subtropical
290        Northwest Pacific. Mar. Ecol. Prog. Ser., 448, 39-49, 2012.

Claustre, H., Bishop, J., Boss, E., Stewart, B., Berthon, J.-F., et al. Bio-optical profiling floats as new observational tools for biogeochemical and ecosystem studies. In Proceedings of the "OceanObs'09: Sustained Ocean Observations and Information for Society" Conference, Venice, Italy, 21-25 September 2009, ed. J Hall, Harrison D.E. and Stammer, D.: ESA Publication WPP-306, 2010.

295  Cullen, J. J.: Subsurface Chlorophyll Maximum Layers: Enduring Enigma or Mystery Solved? Annu. Rev. Mar. Sci., 7, 207–239, 2015.

Du, C., Liu, Z., Kao, S. J. and Dai, M.: Diapycnal fluxes of nutrients in an oligotrophic oceanic regime: the South China Sea. Geophys. Res. Lett., 44, 11510–11518, 2017.

Dunnavan, G. M. and Diercks, J. W.: An analysis of Super Typhoon Tip (October 1979). Mon. Weather Rev., 108, 1915–1923, 1980.

300

Elsner, J. B., Kossin, J. P. and Jagger, T. H.: The increasing intensity of the strongest tropical cyclones. Nature, 455, 92–95, 2008.

Emanuel, K. A.: Thermodynamic control of hurricane intensity. Nature, 401, 665–669, 1999.

Emanuel, K. A.: Increasing destructiveness of tropical cyclones over the past 30 years. Nature, 436, 686–688, 2005.

305  Frank, N. L. and Husain, S. A.: Deadliest tropical cyclone in history. Bull. Am. Meteorol. Soc., 52, 438–444, 1971.

Gierach, M. M., and Subrahmanyam, B.: Biophysical responses of the upper ocean to major Gulf of Mexico hurricanes in 2005. J. Geophys. Res., 113, C04029, 2008.

Glenn, S., Miles, T., Seroka, G., Xu, Y., Forney, R., Yu, F., Roarty, H., Schofield, O. and Kohut, J.: Stratified coastal ocean interactions with tropical cyclones. Nature Communications, 7, 10887, 2016.

310  Gong, X., Jiang, W. S., Wang, L. H., Gao, H. W., Boss, E., Yao, X. H., Kao, S. J. and Shi, J.: Analytical solution of the nitracline with the evolution of subsurface chlorophyll maximum in stratified water columns. Biogeosciences, 14, 2371–2386, 2017.

Graff, J. R., Westberry, T. K., Milligan, A. J., Brown, M. B., Dall'Olmo, G., Van Dongen-Vogels, V. et al. Analytical phytoplankton carbon measurements spanning diverse ecosystems. Deep Sea Res. I, 102, 16–25, 2015.

315  Gray, W. M.: Global view of the origin of tropical disturbances and storms. Mon. Weather Rev., 96, 669–700, 1968.

Han, G., Ma, Z. and Chen, N.: Hurricane Igor impacts on the stratification and phytoplankton bloom over the Grand Banks. J. Mar. Syst., 100–101, 19–25, 2012.

He, J. and Soden, B. J.: Anthropogenic weakening of the tropical circulation: the relative roles of direct CO2 forcing and sea surface temperature change. J. Clim., 28, 8728–8742, 2015.

320  Huang, S. M. and Oey, L. Y.: Right-side cooling and phytoplankton bloom in the wake of a tropical cyclone. J. Geophys. Res., 120, 5735–5748, 2015.

Jacob, S. D., Shay, L. K., Mariano, A. J., and Black, P. G.: The 3D oceanic mixed layer response to Hurricane Gilbert, J. Phys. Oceanogr., 30(6), 1407–1429, 2000.

Johnson, K. S. and Claustre, H.: Bringing Biogeochemistry into the Argo Age. Eos, 97, 11–15, 2016.

325  Kang, S.-W., Jun, K.-C., Park, K.-S. and Han, S.-D.: Storm surge hindcasting of Typhoon Maemi in Masan Bay, Korea. Marine Geod., 32, 218–232, 2009.

Kara, A. B., Rochford, P. A. and Hurlburt, H. E.: An optimal definition for ocean mixed layer depth. J. Geophys. Res., 105(C7), 16803, 2000.

Kossin, J. P.: A global slowdown of tropical-cyclone translation speed. Nature, 558, 104–107, 2018.

330  Letelier, R. M., Karl, D. M., Abbott, M. R. and Bidigare, R. R.: Light driven seasonal patterns of chlorophyll and nitrate in the lower euphotic zone of the North Pacific Subtropical Gyre. Limnol. Oceanogr., 49, 508–519, 2004.

Lin, I. I.: Typhoon-induced phytoplankton blooms and primary productivity increase in the western North Pacific subtropical ocean. J. Geophys. Res., 117, C03039, 2012.

Lin, I. I., and Chan, J. C.: Recent decrease in typhoon destructive potential and global warming implications. Nature
335  Communications, 6(1), 7182–7182, 2015.

Lin, I. I., Pun, I. F. and Wu, C. C.: Upper-ocean thermal structure and the western North Pacific category-5 typhoons. Part II: Dependence on translation speed, Mon. Weather Rev., 137, 3744–3757, 2009.

Lin, S., Zhang, W. Z., Shang, S. P. and Hong, H. S.: Ocean response to typhoons in the western North Pacific: Composite results from Argo data. Deep-Sea Res. I, 123, 62–74, 2017.

340  Liu, H., Hu, Z., Huang, L., Huang, H., Chen, Z., Song, X., Ke, Z. and Zhou, L.: Biological response to typhoon in northern South China Sea: A case study of "Koppu". Cont. Shelf Res., 68, 123–132, 2013.

Mei, M., Lien, C. C., Lin, I. I. and Xie, S. P.: Tropical cyclone-induced ocean response: a comparative study of the South China Sea and Tropical Northwest Pacific. J. Clim., 28, 5952–5968, 2015.

Mignot, A., Claustre, H., Uitz, J., Poteau, A., D'Ortenzio, F. and Xing, X.: Understanding the seasonal dynamics of
345  phytoplankton biomass and the deep chlorophyll maximum in oligotrophic environments: A Bio-Argo float investigation. Global Biogeochem. Cycles, 28, 856–876, 2014.

Needham, H. F., Keim, B. D. and Sathiaraj, D.: A review of tropical cyclone-generated storm surges: global data sources, observations, and impacts. Rev. Geophys., 53, 545–591, 2015.

Pan, S., Shi, J., Gao, H., Guo, X., Yao, X. and Gong, X.: Contributions of physical and biogeochemical processes to
350  phytoplankton biomass enhancement in the surface and subsurface layers during the passage of typhoon Damrey. J Geophys Res Biogeosci., 122, 212–229, 2017.

Platt, T.: Primary production of the ocean water column as a function of surface light intensity: algorithms for remote sensing. Deep Sea Res. I, 33, 149–163, 1986.

Pothapakula, P. K., Osuri, K. K., Pattanayak, S., Mohanty, U. C., Sil, S., and Nadimpalli, R.: Observational perspective of SST
355  changes during life cycle of tropical cyclones over Bay of Bengal. Nat. Hazards, 88(3), 1769–1787, 2017.

Price, J. E., Sanford, J. B., and Forristall, G. Z.: Forced stage responses to a moving hurricane, J. Phys. Oceanogr., 24(2), 233–260, 1994.

Price, J. F.: Upper ocean response to a hurricane. J. Phys. Oceanogr., 11, 153–175, 1981.

Webster, P. J., Holland, G. J., Curry, J. A. and Chang, H.: Changes in Tropical Cyclone Number, Duration, and Intensity in a
360      Warming Environment. Science, 309, 1844–1846, 2005.

Sanford, T. B., Price, J. F. and Girton, J. B.: Upper ocean response to Hurricane Frances (2004) observed by profiling EM-
         APEX floats. J. Phys. Oceanogr., 41, 1041–1056, 2011.

Shang, S., Li, L., Sun, F., Wu, J., Hu, C., Chen, D., Ning, X., Qiu, Y., Zhang, C. and Shang, S.: Changes of temperature and
         bio-optical properties in the South China Sea in response to Typhoon Lingling, 2001. Geophys. Res. Lett., 35, L10602,
365      2008.

Shibano, R., S., Yamanaka, Y., Okada, N., Chuda, T., Suzuki, S. and Niino, H.: Responses of marine ecosystem to typhoon
         passages in the western subtropical North Pacific. Geophys. Res. Lett., 38, L18608, 2011.

Sobel, A. H., Camargo, S. J., Hall, T. M., Lee, C. Y., Tippett, M. K. and Wing, A. A.: Human Influence on Tropical Cyclone
         Intensity. Science, 353(6296), 242–246, 2016.

370   Sriver, R. L. and Huber, M.: Observational evidence for an ocean heat pump induced by tropical cyclones. Nature, 447, 577–
         580, 2007.

Sun, L., Yang, Y., Xian, T., Lu, Z. and Fu, Y.: Strong enhancement of chlorophyll a concentration by a weak typhoon. Mar.
         Ecol. Prog. Ser., 404, 39–50, 2010.

Vecchi, G. A. and Soden, B. J.: Effect of remote sea surface temperature change on tropical cyclone potential intensity. Nature,
375      450, 1066–1070, 2007.

Wu, R. and Li, C.: Upper ocean responses to the passage of two sequential typhoons, Deep Sea Res. I, 132, 68–79, 2018.

Yang, Y. J., Sun, L., Liu, Q., Xian, T. and Fu, Y.: The biophysical responses of the upper ocean to the typhoons Namtheun
         and Malou in 2004. Int. J. Remote Sens., 31(17), 4559–4568, 2010.

Ye, H. J., Sui, Y., Tang, D. L. and Afanasyev, Y. D.: A Subsurface Chlorophyll a Bloom Induced by Typhoon in the South
380      China Sea. J. Mar. Syst., 128, 138–145, 2013.

Zhao, H., Tang, D. and Wang, Y.: Comparison of phytoplankton blooms triggered by two typhoons with different intensities
         and translation speeds in the South China Sea. Mar. Ecol. Prog. Ser., 365, 57–65, 2008.

Zhao, H., Pan, J., Han, G., Devlin, A. T., Zhang, S. and Hou, Y.: Effect of a fast-moving tropical storm Washi on phytoplankton
         in the northwestern South China Sea. J. Geophys. Res., 122, 3404–3416, 2017.

385   Zhang, H., Wu, R., Chen, D., Liu, X., He, H., Tang, Y. et al. Net modulation of upper ocean thermal structure by Typhoon
         Kalmaegi (2014). J. Geophys. Res., 122, 7154–7171, 2018.

Zheng, G. and Tang, D.: Offshore and nearshore chlorophyll increases induced by typhoon winds and subsequent terrestrial
         rainwater runoff. Mar. Ecol. Prog. Ser., 333, 61–74, 2007.

Zheng, Z.-W., Ho, C.-R. and Kuo, N.-J.: Importance of pre-existing oceanic conditions to upper ocean response induced by
390      Super Typhoon Hai-Tang, Geophys. Res. Lett., 35, L20603, 2008.

Zhou, L., Tan, Y., Huang, L., Huang, J., Liu, H., and Lian, X.: Phytoplankton growth and microzooplankton grazing in the continental shelf area of northeastern South China Sea after Typhoon Fengshen. Continental Shelf Research, 31(16), 1663–1671, 2011.
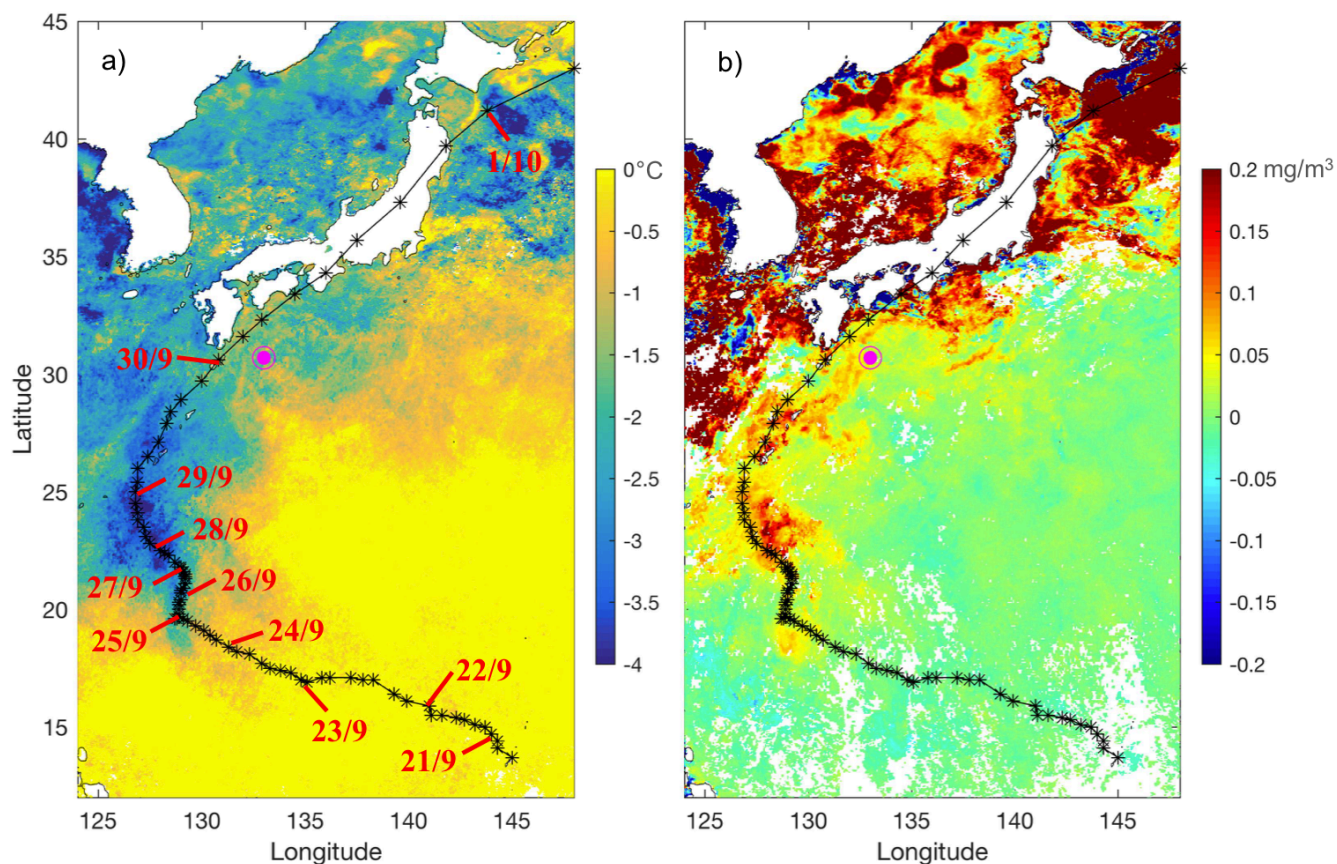
**Figure 1: The differences in averaged sea surface temperature (a) and chlorophyll (b) measured during the period of September 10 to September 30 versus that measured between October 1 to October 20. The remote sensing observations are obtained as the MODIS L3 daily data. The trajectory of Typhoon Trami is shown as black curve with its central location every 3-hour labels as asterisks and the date is labelled for the location at noon (UTC). The location of BGC-Argo on September 30 is shown as magenta symbol.**
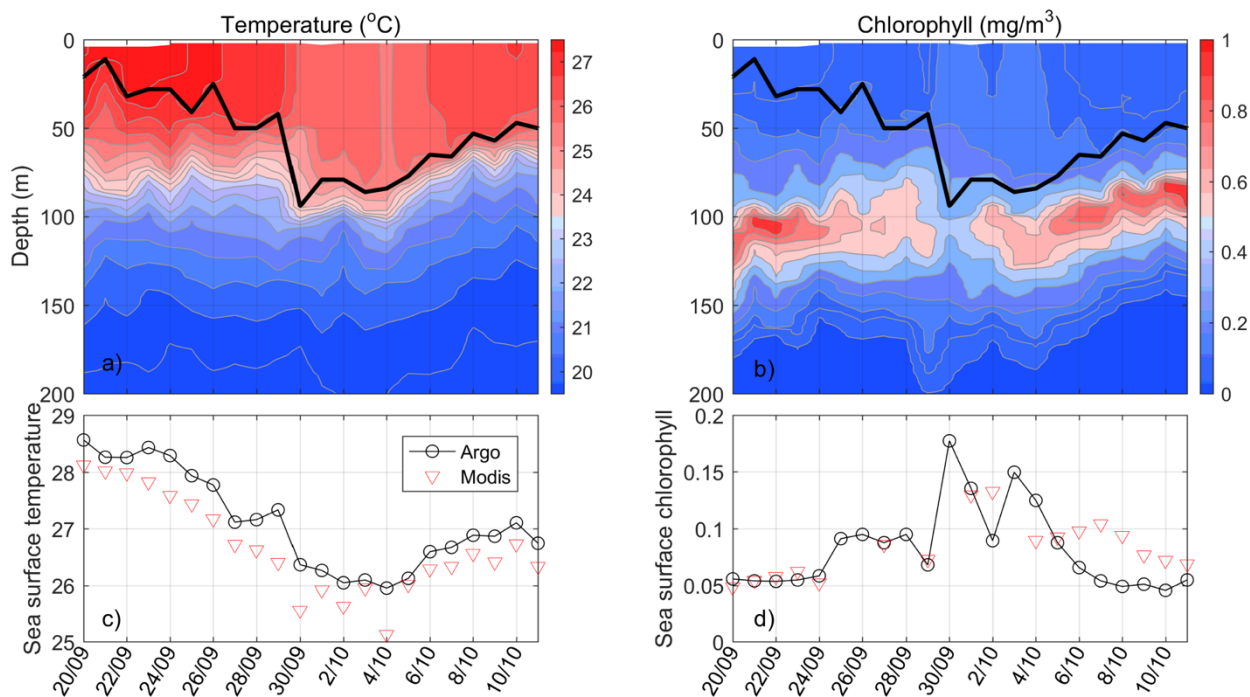
**Figure 2: Profiles of temperature (a) and chlorophyll (b) captured by the biogeochemical-Argo (BGC-Argo); superposed as the thick black curve is the mixed layer depth (MLD). Comparison between the sea surface temperature (c) and chlorophyll (d) from the BGC-Argo and remote sensing observations. Typhoon Trami passed nearby the BGC-Argo on September 30, 2018.**

405
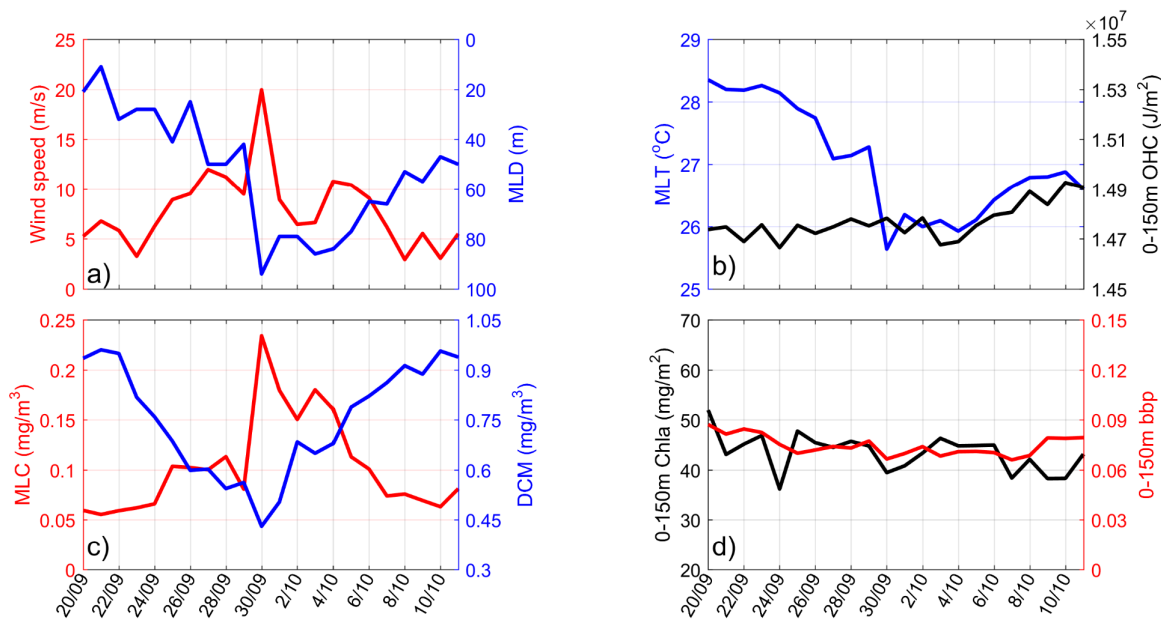
410

**Figure 3:** Time series of (a) wind speed and MLD at the BGC-Argo, (b) mean temperature above the MLD (MLT) and integrated ocean heat content (OHC) between 0 and 150 m, (c) mean chlorophyll above the MLD (MLC) and deep chlorophyll maximum (DCM), and (d) integrated chlorophyll and bbp between 0 and 150 m.
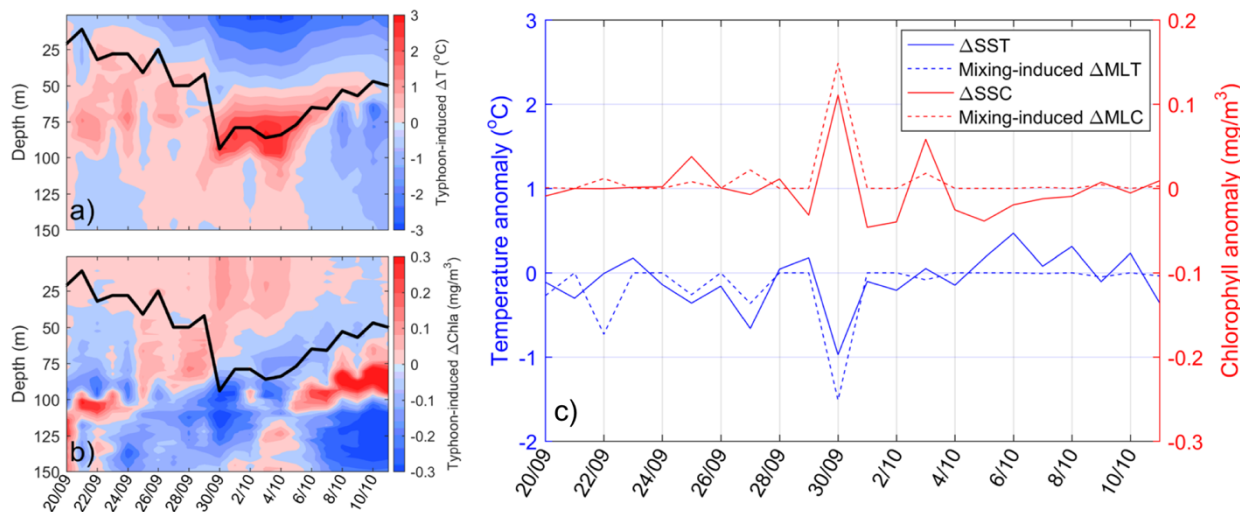
415

**Figure 4:** Profiles of typhoon-induced changes of (a) temperature and (b) chlorophyll concentration. The changes were calculated for each day's profile by subtracting the averaged profile from seven days prior to September 20 (i.e., September 13 to 19). (c) Time series of the change in sea surface temperature (ΔSST, solid blue), mixing-induced change in MLT (dashed blue), sea surface chlorophyll concentration (ΔSSC, solid red) and mixing-induced change in MLC (dashed red).
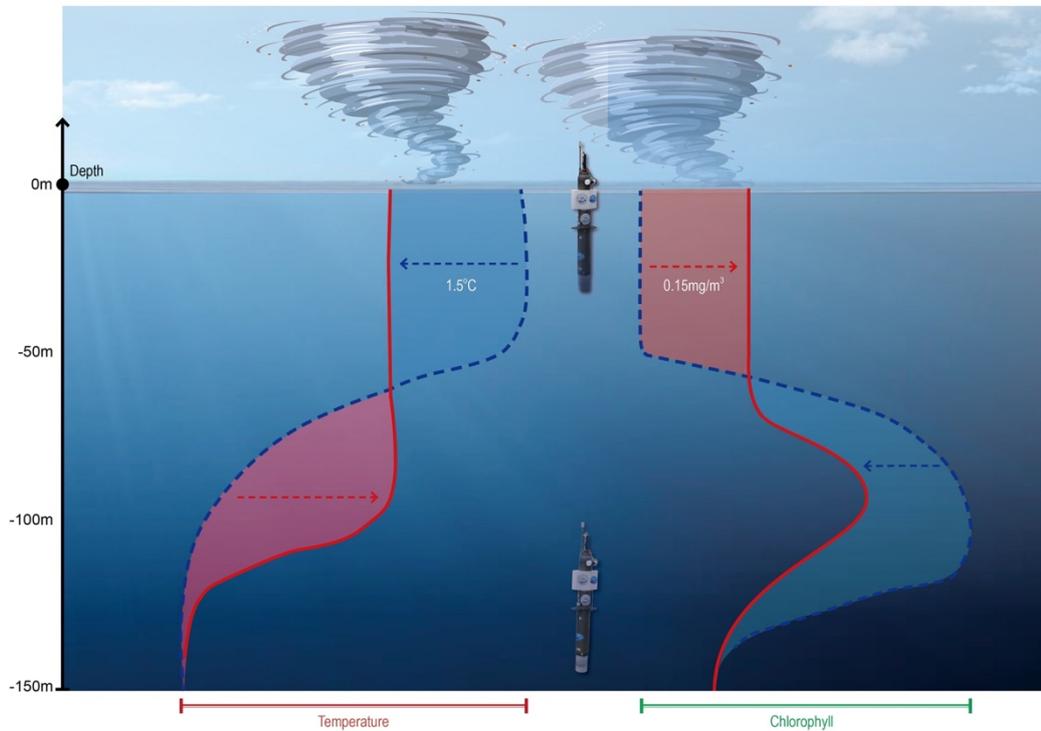
420

**Figure 5: Schematic diagram for typhoon's impact on the vertical distribution of temperature (left) and chlorophyll (right).**